Supporting Information

Two-Dimensional Fluorescence and Chemiluminescence Orthogonal Probe for Discriminating and Quantifying Similar Proteins

Juan Li,[a] Xiuyan Zhao,[a] Yutao Zhang,[a,*] Yao Lu,[a] Haoyun Xue,[a] Dan Li,[a] Qiang Liu,[a] Chenxu Yan,[a] Weijie Chi,[b] Xingqing Xiao,[b,*] Wei-Hong Zhu,[a] and Zhiqian Guo[a,*]

[a] Key Laboratory for Advanced Materials and Institute of Fine Chemicals, Feringa Nobel Prize Scientist Joint Research Center, Frontiers Science Center for Materiobiology and Dynamic Chemistry, Shanghai Frontiers Science Center of Optogenetic Techniques for Cell Metabolism, State Key Laboratory of Bioreactor Engineering, School of Chemistry and Molecular Engineering, East China University of Science and Technology, Shanghai 200237, China.

[b] Department of Chemistry, School of Chemistry and Chemical Engineering, Hainan University, Haikou City, Hainan Province 570228, China.

* Email: zhangyutao@ecust.edu.cn (Y. Z.), xqxiao@hainanu.edu.cn (X. X.), guozq@ecust.edu.cn (Z. G.)

Contents

1. Experimental Section

Materials and General Methods

Unless special stated, all solvents and chemicals were purchased from commercial suppliers in analytical grade and used without further purification. The ^{1}H and ^{13}C NMR spectra were recorded on a Bruker AM 400 spectrometer, using TMS as an internal standard. High-resolution mass spectrometry data were obtained with a Waters LCT Premier XE spectrometer. Absorption spectra were collected on a Varian Cary 500 spectrophotometer, and fluorescence spectra measurements were performed on a Varian Cary Eclipse fluorescence spectrophotometer. The LED white light was purchased from FENIX Inc. We also used the optical power meter to carefully measure the average light intensity (21 mW cm^{-2}) in our experimental conditions. Chemiluminescence signals in 96-well plates were recorded using an ImageQuant LAS4000 system. Each well intensity of 96-well plates was quantified using the ImageQuant TL software. Fluorescence lifetimes were obtained using an Edinburgh FLS1000 fluorescence spectrometer. Femtosecond transient absorption (TA) spectra were collected using a commercial femtosecond transient absorption spectrometer (Helios fire, Ultrafast System). Confocal fluorescence images were taken on a Leica TCS SP8 (63 × oil lens). Chemiluminescence spectra, *in vivo* chemiluminescence and fluorescence images were measured with a PerkinElmer IVIS Spectrum Imaging System.

General Procedure for Spectral Measurements

A stock solution of 1 mM was made by dissolving the probe in analytically pure dimethyl sulfoxide. This stock solution was then diluted to 10 μM with a mixture (v/v 3:7) of DMSO and phosphate buffer (PBS, pH 7.4). All optical experiments were performed in a mixture (v/v 3:7) of DMSO and phosphate buffer (PBS, pH 7.4). For titration experiments, a certain concentration of HSA or BSA was added to a total volume of 2.0 mL of the probe (10 μM) solution. The resulting solution was shaken well and then incubated at 37 °C for 40 min, followed by spectroscopic measurements. For the fluorescence lifetime test, the probe concentration was 20 μM and the concentration of both HSA and BSA was 200 μg/mL. The absorption spectra of probe were recorded in the range of 300–700 nm. The fluorescence spectra of the probe in the solvents, PBS buffer and presence of proteins were recorded in the range of 535–800 nm with the excitation wavelength (λ_{ex}) of 500 nm. In all experiments, the samples were contained in a 1-cm-path-length quartz cell, and the measurements were conducted at 25 °C.

Detection of HSA in Human Urine

Urine was sampled from the samples collected at the hospital on the same day. These samples were transported refrigerated to the laboratory shire and tested immediately afterward. After adding 20 μL of 1 mM probe solution to the mixture of 30% DMSO, 35% Tris-HCl (pH 8.8), and 35% urine, the samples were incubated at 37 °C for 40 min and then tested. The standard working curve in urine was also measured in this system, using 0-10 μM probe and healthy human urine.

Cell Experiment

Cell Lines

The human epithelioid cervical carcinoma cell line HeLa was purchased from the Institute of Cell Biology (Shanghai, China). Cells were all propagated in T-75 flasks cultured at 37 ^{o}C under a humidified 5% CO_2 atmosphere in DMEM medium (GIBCO/Invitrogen, Camarillo, CA, USA), which were supplemented with 10 % fetal bovine serum (FBS, Biological Industry, Kibbutz Beit Haemek, Israel) and 1 % penicillin-streptomycin (10,000 U mL^{-1} penicillin and 10 mg/ml streptomycin, Solarbio life science, Beijing, China).

In Vitro Cytotoxicity Assay

The cell cytotoxicity of DCM-SA to Hepg 2 cells was measured by 3-(4, 5-dimethylthiazol-2-yl)-2, 5-diphenyltetrazolium bromide (MTT) assay. Cells were plated in 96-well plates in 0.1 mL volume of DMEM medium without 10 % FBS, at a density of 1×10^4 cells/well and added with desired concentrations of DCM-SA. After incubation for 24 h, change the culture solution to DMSO and continue for 3-4 hours. Absorbance was measured at 510 nm with a Tecan GENios Pro multifunction reader (Tecan Group Ltd., Maennedorf, Switzerland). Each concentration was measured in triplicate and used in three independent experiments. The relative cell viability was calculated by the equation: cell viability (%) = $(OD_{treated}/OD_{control}) \times 100\%$.

In Vitro Cellular Fluorescence Imaging

The Hepg 2 cells were seeded onto glass-bottom petri dishes with complete medium (1.5 mL) for 12 h. The cells pro-incubated with 200 μg/mL HSA, 200 μg/mL BSA for 1 h, respectively. Then, these cells were incubated with 10 μM DCM-SA after wishing by PBS (pH 7.4) for three times. A control group was set up with only 1 h incubation with the probe. Before imaging, wash cells for three times to clean the background. The images were then photographed by using a confocal laser scanning microscope Leica TCS SP8 (63 × oil lens) with 500 nm as the excitation wavelength and 610-650 nm as the emission wavelength.

In Vitro Cellular Chemiluminescence Imaging in 96-Well Plates

The Hepg 2 cells at 1×10^5 cells/well were placed into the wells of a black 96-well plate with complete medium (100 μL) for 12 h. The cells pro-incubated with 200 μg/mL HSA, 200 μg/mL BSA for 1 h, respectively. Then, these cells were pro-incubated with 50 μM DCM-SA for 24 h. Cells were washed with PBS (pH 7.4) for 3 times and immediately imaged with or without irradiation (15 s, 21 $mW\cdot cm^{-2}$) using an ImageQuant LAS4000 system (acquisition time of 5 min).

Molecular docking

AutoDock Vina program, which was developed based on a combination of heuristic search algorithm and physics-based score function, is conducted to predict the ways by which the small molecules DCM-SA and DPY can interact with the two mammalian serum albumins HSA and BSA. In this

docking study, the small molecules DCM-SA and DPY are set as ligands, and the serum albumins HSA and BSA are treated as rigid receptors. A cubic grid box with the sizes of (size_*x*, size_*y*, size_*z*) = (70 Å, 70 Å, 70 Å) is used to envelop the whole serum albumins to examine potential active pockets. Starting from different random seeds, three independent docking attempts are done to search for all possible binding modes referring to four HSA/DCM-SA, BSA/DCM-SA, HSA/DPY, and BSA/DPY complexes. As a result, some putative binding poses can be obtained. Relevant information of experiments, such as different fluorescence and chemiluminescence of HSA and BSA, is taken as essential clues to check and eliminate those impossible binding poses. All the remaining binding poses are subjected to atomistic molecular dynamics (MD) simulations to determine the most likely binding structures of the small molecules DCM-SA and DPY with the serum albumins HSA and BSA.

Quantum Mechanics Calculation and Atomistic Molecular Dynamics Simulation

Firstly, quantum mechanics calculations are performed on the two small molecules DCM-SA and DPY using the Gaussian16 package to obtain their partial atomic charges for binding study. The geometry optimization and electrostatic surface potential calculation of DCM-SA and DPY are implemented using the Hartree-Fock method with the 6-31G(d) basis set. Later, a two-stage restrained electrostatic surface potential protocol is followed to fit the partial atomic charges of the two small molecules. It is worth noting that the total charge of DCM-SA is neutral, but the total charge of DPY is -1.

Atomistic MD simulations with explicit solvent are carried out in 100 ns to examine the thermodynamic stability of these docking complexes. The amber GAFF2 force field is used to describe the DCM-SA and DPY, and the protein ff19SB force field is applied for the HSA and BSA. Each individual complex is solvated fully into a periodic truncated octahedral box with at least 12 Å buffer of OPC water molecules surrounding this complex. Sodium counterions (Na^+) are added to neutralize the entire system. Temperature and pressure are controlled at 300 K and 1 bar, respectively, during the simulations. The particle mesh Ewald method is used to compute long-ranged electrostatic interactions, and the van der Waals interactions are cut off at 8 Å. The SHAKE algorithm is applied to constrain the motions of hydrogen bond. A clustering analysis is performed on the last 5 ns simulation trajectories to determine a representative structure that reflects the most likely binding state of the small molecules DCM-SA and DPY with the serum albumins HSA and BSA in nature. Each atomistic MD simulation contains four phases: (1) an energy minimization is performed using 500 steps of steepest descent followed by 500 steps of the conjugate gradient to relax water molecules only; (2) another energy minimization is performed using 1000 steps of steepest descent followed by

1500 steps of the conjugate gradient to relax the whole system; (3) a 45-ps isothermal-isobaric (NPT) ensemble simulation is carried out in four substeps to gradually heat the system from 0 K to 300 K; (4) a 100-ns production simulation is conducted in the canonical (NVT) ensemble to reach an equilibrated state at the end.

Calculation of binding free energy with the var-MM/GBSA approach

Binding free energy of a small molecule and a serum albumin is calculated using the MM/GBSA approach, expressed as the Equation S-1:

$$\Delta G_{binding} = G_{TOT}^{complex} - G_{TOT}^{small\ molecule} - G_{TOT}^{serum\ albumin} \quad \text{(S-1)},$$

where $G_{TOT}^{complex}$, $G_{TOT}^{small\ molecule}$ and $G_{TOT}^{serum\ albumin}$ are total free energies of the complex, small molecule, and serum albumin in solution, respectively. The total free energies G_{TOT} of a biomolecule contains enthalpic (*H*) and entropic (*TS*) contributions (Equation S-2)

$$G_{\mathrm{TOT}} = H - TS = U_{\mathrm{INT}} + U_{\mathrm{VDW}} + U_{\mathrm{ELE}} + G_{\mathrm{EGB}} + G_{\mathrm{GBSUR}} - TS \quad \text{(S-2)},$$

where U_{INT}, U_{VDW}, U_{ELE}, G_{EGB} and G_{GBSUR} indicate the internal energy (INT), van der Waals energy (VDW), electrostatic energy (ELE), the polar solvation energy (EGB) and the non-polar solvation energy (GBSUR), and TS is the entropy. The U_{INT} is associated with the vibration of the bonds, bond angles, and dihedral angles. The U_{VDW} is modeled using a typical 12–6 Lennard-Jones equation. The U_{ELE} follows Coulomb's law. The G_{EGB} is calculated based on an implicit-explicit MM/GBSA approach with variable solute internal dielectric constant model (var-MM/GBSA). The G_{GBSUR} is calculated by multiplying the solvent-accessible surface area of solute molecules by the surface tension. The entropy TS is evaluated using normal mode analysis approach.

By introducing Equation S-2 into Equation S-1, we can rewrite the expression as

$$\begin{aligned}\Delta G_{binding} = & \sum_{i \in small\ molecule} \sum_{j \in serum\ albumin} U_{VDW}(i,j) + \sum_{i \in small\ molecule} \sum_{j \in serum\ ablun} \\ & + \sum_{i \in small\ molecule} \sum_{i' \in small\ molecule} \left(G_{EGB}^{complex}(i,i') - G_{EGB}^{small\ molecule}(i,i')\right) \\ & + \sum_{j \in serum\ albumin} \sum_{j' \in serum\ albumin} \left(G_{EGB}^{complex}(j,j') - G_{EGB}^{serum\ albumin}(j,j')\right) \\ & + \left(G_{GBSUR}^{complex} - G_{GBSUR}^{small\ molecule} - G_{GBSUR}^{serum\ albumin}\right)\end{aligned}$$

$$- (TS_{GBSUR}^{complex} - TS_{GBSUR}^{small\ molecule} - TS_{GBSUR}^{serum\ albumin}) \quad \text{(S-3)}.$$

The first two terms in Equation S-3 are the intermolecular VDW and the intermolecular charge-charge (ELE+EGB) interactions between a small molecule and a serum albumin. The third term refers to the difference in the intramolecular EGB interaction of a small molecule when within the complex and alone in solution. The fourth term refers to the difference in the intramolecular EGB interaction of serum albumin when within the complex and alone in solution. The fifth and sixth terms reflect the difference in the GBSUR and TS contributions between the complex, small molecule, and serum albumin prior to binding.

Surface Plasmon Resonance (SPR)

Surface plasmon resonance (SPR) measurements were performed on a Biacore 8K instrument at 25 ^{o}C. HSA or BSA was captured on streptavidin-coated CM5 sensor chips in the flow channels until approximately 7000 response unit (RU) was achieved. Next, the reference and modified flow cells were washed with three consecutive injections of a mixture solution of 50% isopropanol and 1 M NaCl in 50 mM NaOH. A mixture solution composed of PBS (10 mM, pH 7.4), 5% DMSO and 0.05% Tween-20 was used as the running buffer for the immobilization, and kinetic studies of the interaction of DCM-SA with HSA and BSA, respectively. Kinetic study of the interaction of DPY with HSA and BSA was also performed. Analytes were dissolved in PBS buffer (10 mM, pH 7.4) containing 5% DMSO and 0.05% Tween-20, and a flow rate of 30 μL/min was employed for association and dissociation for 120 s at a constant temperature of 25 ^{o}C. Using BiacoreTM Insight Evaluation Software 4.0, the response curves of various analyte concentrations were globally fitted by a 1:1 Langmuir binding model. The black line is the fitting curve.

2. Synthetic Method

Compounds 1-6 were synthesized according to the previous report[22].

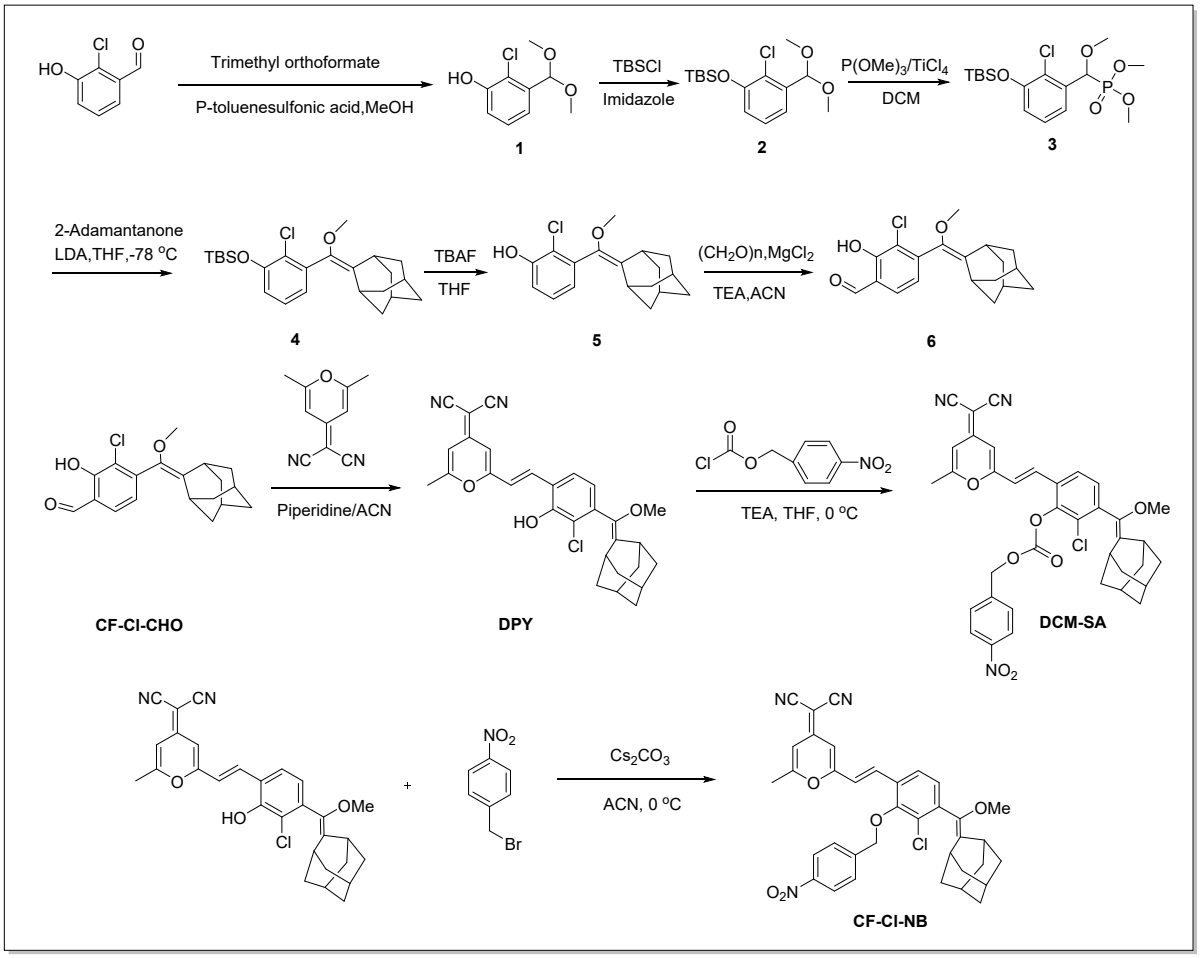

Scheme S1. Synthetic route of **DPY**, **DCM-SA** and **CF-Cl-NB.**

Synthesis of DPY

4-(dicyanomethylene)-2,6-dimethyl-4H-pyran (128 mg, 0.70 mmol), CF-Cl-CHO (224 mg, 0.67 mmol), acetonitrile (25 mL), and piperidine (0.5 mL) were added to a 100 mL dry double-necked flask. The mixture was refluxed for 6 h, cooled and then rotary evaporated to remove the organic solvent. The mixture was purified by silica gel column chromatography using PE/EA (v/v, 65:35) to give orange-red solid (35 mg, yield: 11%). ^{1}H-NMR (400 MHz, $CDCl_3$, ppm): δ 7.66 (d, 1 H, J = 16 Hz, -Alkene-H), 7.39 (d, 1 H, J = 8 Hz, -Ph-H), 6.94 (d, J = 16 Hz, 1 H, -Alkene-H), 6.91 (d, J = 7.6 Hz, 1 H, -Ph-H), 6.71 (d, 1 H, J = 2 Hz, -Pyran-H), 6.56 (d, 1 H, J = 1.2 Hz, -Pyran-H), 6.28 (s, 1 H, -OH), 3.33 (s, 3 H, -O-***CH₃***), 3.28 (s, 1 H, -Adamantane-H), 2.43 (s, 3 H, -***CH₃***), 2.14 (s, 1 H, -Adamantane-H), 1.97-1.77 (m, 12 H, -Adamantane-H). ^{13}C-NMR (100 MHz, $CDCl_3$, ppm): δ 158.32, 155.95, 150.45, 139.33, 136.73, 132.54, 126.24, 123.99, 123.88, 122.11, 121.66, 120.10, 115.22, 107.65, 60.07, 57.45, 39.16, 37.01, 32.98, 29.76, 28.24. Mass spectrometry (ESI-MS, m/z): [M - H]$^{-}$

calcd for $C_{29}H_{26}ClN_2O_3$, 485.1626; found, 485.1642.

Synthesis of compound DCM-SA

DPY (40 mg, 0.08 mmol) and TEA (18 μL, 0.13 mmol) were added to a 100 mL dry double-necked flask and dissolved in 20 mL of super-dry tetrahydrofuran. After the reaction liquid is cooled to 0 °C, 4-nitrobenzyl chloroformate is added drop by drop. Then bring it to room temperature and stir for 24 h. After the reaction, the solvent was evaporated under reduced pressure and column chromatography was performed (EA:PE = 2:8). Yellow solid was obtained (25 mg, yield 47 %). ^{1}H-NMR (400 MHz, $CDCl_3$, ppm): δ 8.24 (d, 2 H, J = 8.4 Hz, -Ph-H), 7.62 (d, 2 H, J = 8.4 Hz, -Ph-H), 7.54 (d, 1 H, J = 8.0 Hz, -Ph-H), 7.45 (d, 1 H, J = 16.4 Hz, -Alkene-H), 7.30 (d, 1 H, J = 8.0 Hz, -Ph-H), 6.80 (d, 1 H, J = 16 Hz, -Alkene-H), 6.69 (s, 1 H, -Pyran-H), 6.56 (s, 1 H, -Pyran-H), 5.43 (s, 2 H, -C$\boldsymbol{H_2}$-), 3.32 (s, 3 H, -O-$\boldsymbol{CH_3}$), 3.28 (s, 1 H, -Adamantane-H), 2.38 (s, 3 H, -C$\boldsymbol{H_3}$), 2.10 (s, 1 H, -Adamantane-H), 1.97-1.72 (m, 12 H, -Adamantane-H). ^{13}C-NMR (100 MHz, $CDCl_3$, ppm): δ .171.22, 162.21, 157.98, 155.92, 151.81, 148.08, 145.62, 141.44, 138.69, 138.12, 133.89, 130.13, 129.09, 128.73, 126.99, 125.19, 123.93, 123.68, 122.07, 114.74, 108.54, 106.65, 69.41, 63.88, 60.49, 57.50, 38.59, 36.94, 32.94, 29.79, 28.24, 21.07, 20.00, 14.20. Mass spectrometry (ESI-MS, m/z): $[M - H]^-$ calcd for $C_{37}H_{31}ClN_3O_7$, 664.1845; found, 664.1867.

Synthesis of CF-Cl-NB

DPY (31 mg, 0.064 mmol) and cesium carbonate (32 mg, 0.10 mmol) were added into a 50 mL dry two-mouth bottle, dissolved in ACN and cooled to 0 ^{o}C for 20 min. Then 4-nitrobenzene bromide (28 mg, 0.13 mmol) was added. After the reaction was completed, the mixture was diluted with 100 mL EA, washed with 100 mL saturated ammonium chloride solution, dried with anhydrous sodium sulfate, steamed under pressure, and column chromatography (PE: EA = 7:3). Yellow solid was obtained (17 mg, yield 43 %). ^{1}H-NMR (400 MHz, $CDCl_3$, ppm): δ 8.29 (d, 2 H, J = 8.4 Hz, -Ph-H), 7.70 (d, 2 H, J = 7.6 Hz, -Ph-H), 7.61 (d, 1 H, J = 15.2 Hz, -Alkene-H), 7.51 (d, 1 H, J = 8.4 Hz, -Ph-H), 7.18 (d, 1 H, J = 8 Hz, -Ph-H), 6.75 (d, 1 H, J = 16 Hz, -Alkene-H), 6.66 (s, 1 H, -Pyran-H), 6.54 (s, 1 H, -Pyran-H), 5.14 (d, 2 H, J = 5.6 Hz, -C$\boldsymbol{H_2}$-), 3.36 (s, 3 H, -O-$\boldsymbol{CH_3}$), 3.30 (s, 1 H, -Adamantane-H), 2.31 (s, 3 H, -$\boldsymbol{CH_3}$), 2.11 (s, 1 H, -Adamantane-H), 1.98-1.73 (m, 12 H, -Adamantane-H). ^{13}C-NMR (100 MHz, $CDCl_3$, ppm): δ 161.86, 158.30, 155.93, 153.29, 147.93, 143.43, 139.20, 138.58, 133.40, 131.06, 129.68, 129.40, 128.38, 124.60, 123.85, 120.54, 114.74, 108.10, 106.60, 74.46, 60.43, 57.50, 38.72, 36.99, 33.05, 29.78, 28.18, 19.92. Mass spectrometry (ESI-MS, m/z): $[M + Na]^+$ calcd for $C_{36}H_{32}ClN_3O_5Na$, 644.1928; found, 644.1925.

3. Supplementary Figures

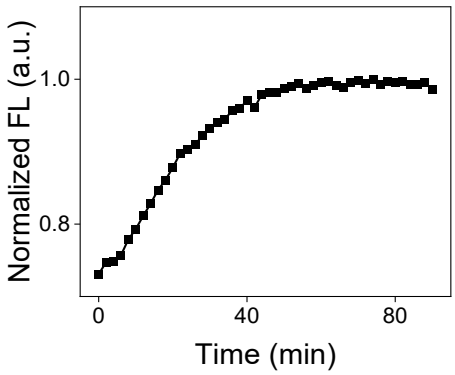

Figure S1. Time dependence of emission spectra (0 - 90 min), λ_{ex} = 500 nm, λ_{em} = 615 nm.

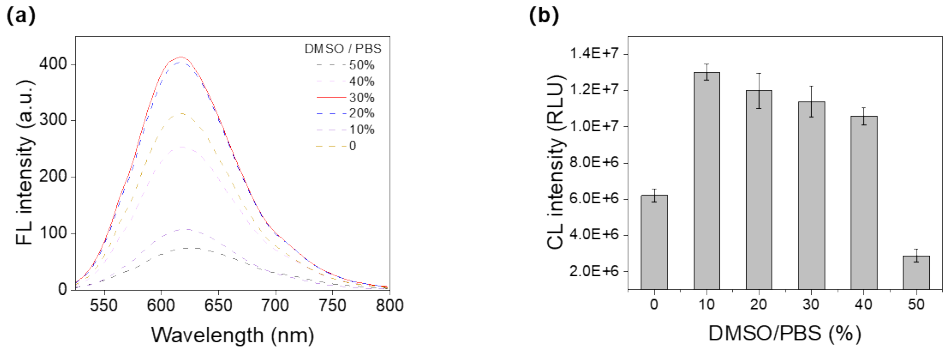

Figure S2. Fluorescence spectra (a) and chemiluminescence intensity (b) of DCM-SA (10 μM) in the presence of HSA (100 μM) in different volume ratios of DMSO/PBS (pH 7.4).

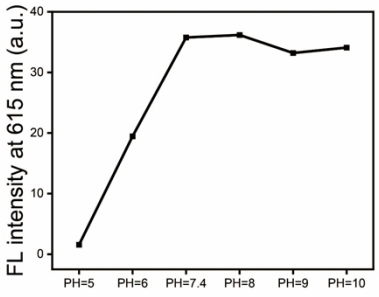

Figure S3. Effects of pH on the fluorescence of DCM-SA (10 μM) in the presence of HSA (80 mg/L). $\lambda_{ex/em}$ = 495 nm/615 nm.

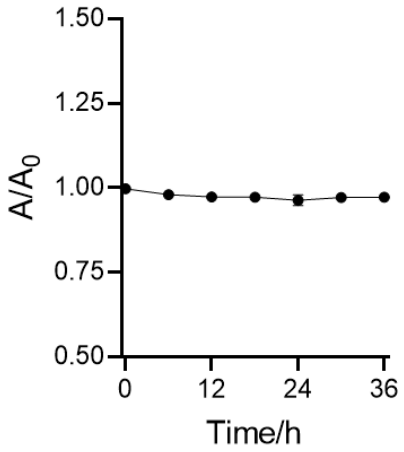

Figure S4. The stability of DCM-SA at room temperature.

Table S1 The relative fluorescence quantum yields of HSA/DPY and BSA/DPY complexes

	HSA/DPY	BSA/DPY
Φ_f [a]	0.184	0.124

[a] The relative fluorescence quantum yield Φ_f value was determined using Rh-B as a reference in a 30% DMSO, 10% 40 mg/mL BSA or HSA, and 60% PBS mixture.

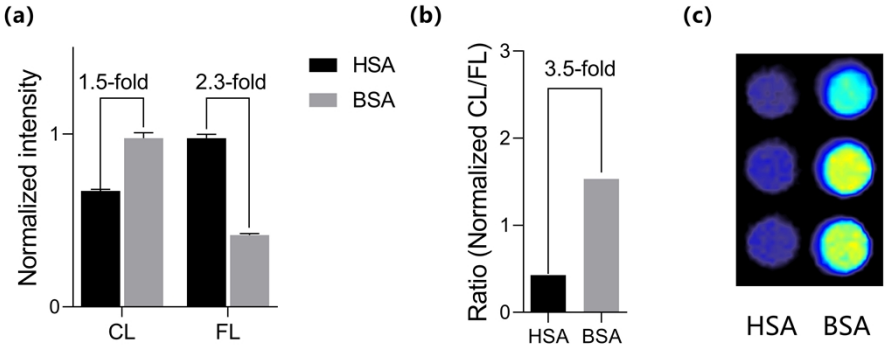

Figure S5. The normalized fluorescence and chemiluminescence intensity (a), the ratio of normalized CL / FL (b), and chemiluminescence image (c) of DCM-SA (10 μM) in the presence of HSA / BSA (10 μM).

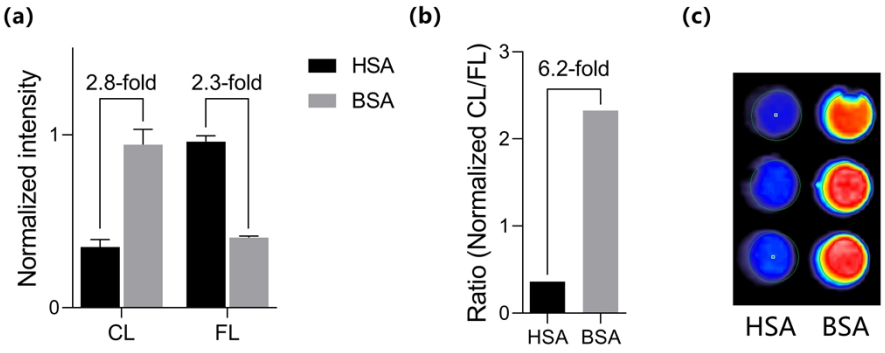

Figure S6. The normalized fluorescence and chemiluminescence intensity (a), the ratio of normalized CL / FL (b), and chemiluminescence image (c) of DCM-SA (10 μM) in the presence of HSA / BSA (20 μM).

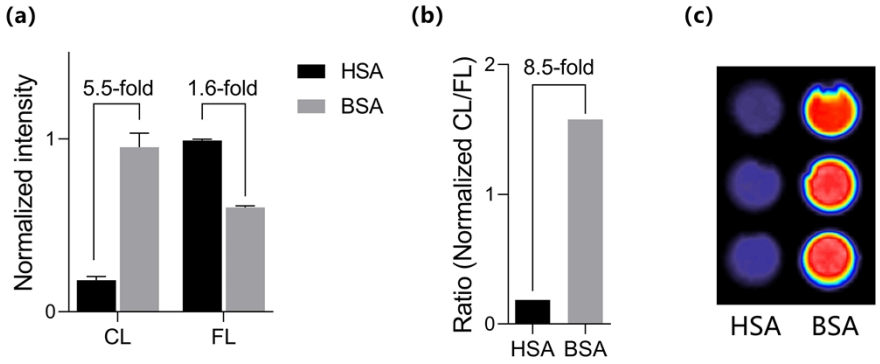

Figure S7. The normalized fluorescence and chemiluminescence intensity (a), the ratio of normalized CL / FL (b), and chemiluminescence image (c) of DCM-SA (10 μM) in the presence of HSA / BSA (100 μM).

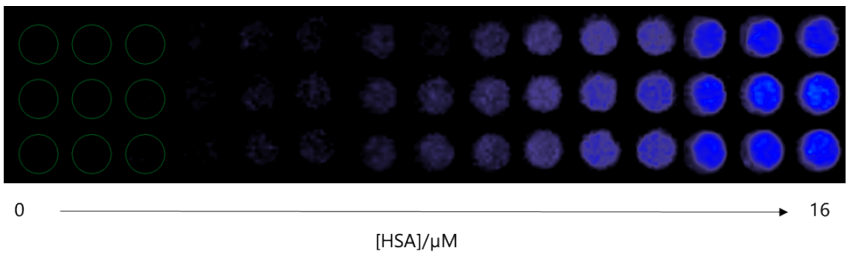

Figure S8. CL imaging of DCM-SA vs HSA concentration.

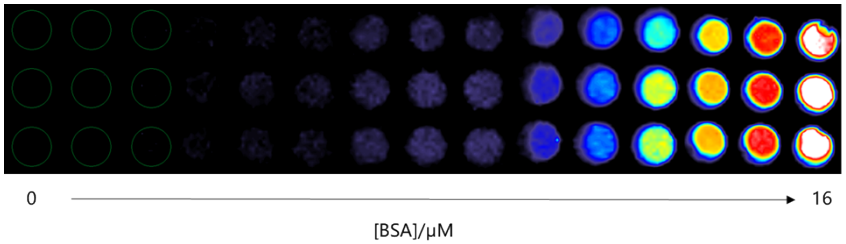

Figure S9. CL imaging of DCM-SA vs BSA concentration.

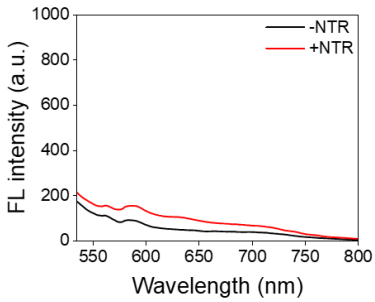

Figure S10. The fluorescence spectra of DCM-SA (10 μM) before and after incubation with NTR (10 μg/mL). λ_{ex} = 500 nm.

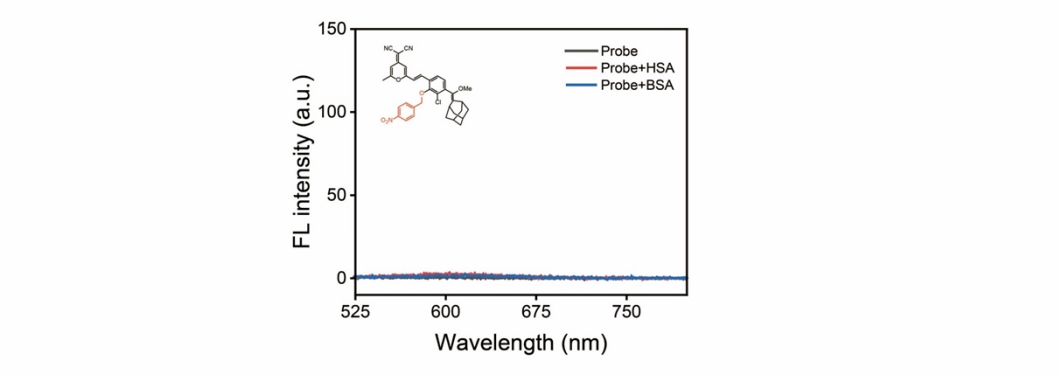

Figure S11. The fluorescence spectra of CF-Cl-NB (10 μM) in the absence and presence of HSA / BSA (20 μM). λ_{ex} =500 nm.

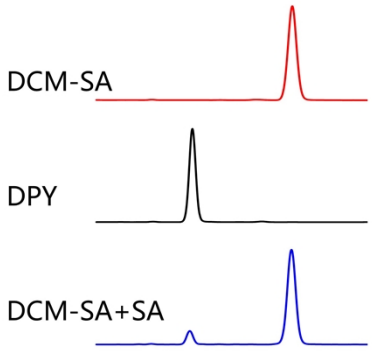

Figure S12. HPLC analysis of DCM-SA after incubation with SA.

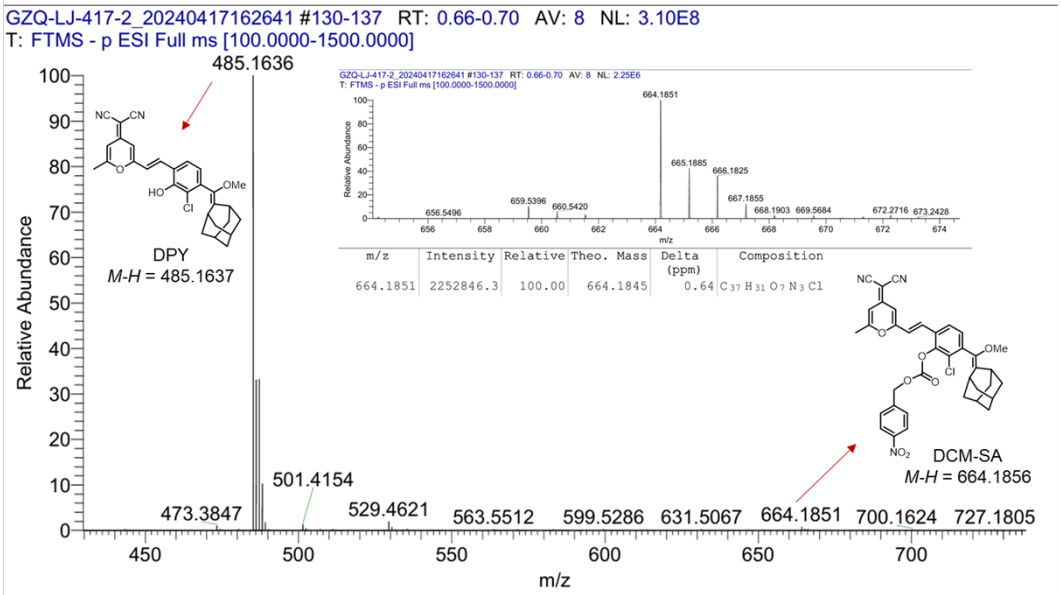

Figure S13. HR-MS spectrum of DCM-SA in the presence of HSA.

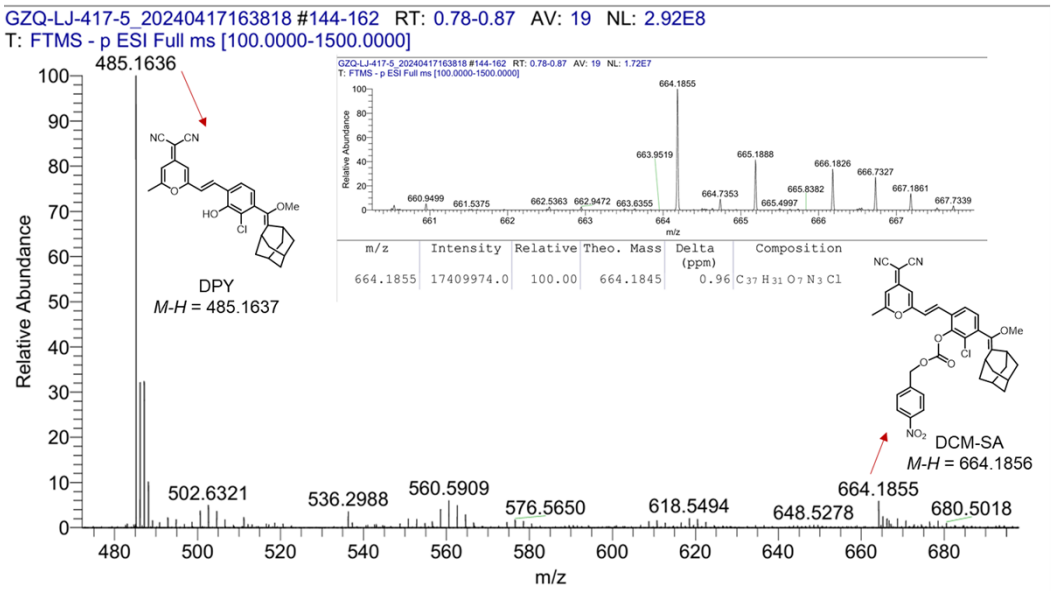

Figure S14. HR-MS spectrum of DCM-SA in the presence of BSA.

Figure S15. Comparison between the sequences of the two serum albumins. Highlighted in red are the primary discrepancies in residue types (hydrophobic, hydrophilic, or charged), and the essential amino acids cysteine (C) and methionine (M) are colored in magenta and blue, respectively.

Table S2. All the atoms of DCM-SA are numbered and assigned to atom types using the GAFF2 force field. The partial atomic charges of DCM-SA are also given in the table.

Atom index	Atom types	Partial charges	Atom index	Atom types	Partial charges	Atom index	Atom types	Partial charges	Atom index	Atom types	Partial charges
1	cc	0.4599	21	ha	0.0972	41	c3	0.4221	61	hc	0.0746
2	cd	-0.5019	22	ca	-0.2151	42	hc	-0.0180	62	c	0.8319
3	ha	0.2031	23	ca	-0.0708	43	c3	-0.5168	63	o	-0.5465
4	cd	0.5539	24	ha	0.1312	44	hc	0.1164	64	os	-0.2958
5	ce	-0.6159	25	ca	-0.2761	45	hc	0.1164	65	c3	0.0295
6	cg	0.5450	26	ha	0.1561	46	c3	-0.5168	66	h1	0.0841
7	n1	-0.5030	27	ca	0.2710	47	hc	0.1164	67	h1	0.0841
8	cg	0.5450	28	ca	-0.2848	48	hc	0.1164	68	ca	0.1073
9	n1	-0.5030	29	cl	-0.0012	49	c3	-0.5168	69	ca	-0.1408
10	cd	-0.5640	30	ca	0.5870	50	hc	0.1164	70	ha	0.1223
11	ha	0.2226	31	os	-0.5047	51	hc	0.1164	71	ca	-0.1315
12	cc	0.5200	32	ce	0.0362	52	c3	-0.5168	72	ha	0.1542
13	c3	-0.5409	33	os	-0.2922	53	hc	0.1164	73	ca	-0.0305
14	hc	0.1677	34	c3	0.1902	54	hc	0.1164	74	no	0.7539
15	hc	0.1677	35	h1	0.0034	55	c3	0.4446	75	o	-0.4212
16	hc	0.1677	36	h1	0.0034	56	hc	-0.0270	76	o	-0.4212
17	os	-0.2886	37	h1	0.0034	57	c3	0.4446	77	ca	-0.1315
18	ce	-0.3760	38	c2	-0.2389	58	hc	-0.0270	78	ha	0.1542
19	ha	0.1943	39	c3	0.4221	59	c3	-0.3748	79	ca	-0.1408
20	cf	0.0853	40	hc	-0.0180	60	hc	0.0746	80	ha	0.1223

Table S3. All the atoms of DPY are numbered and assigned to atom types using the GAFF2 force field. The partial atomic charges of DCM-SA are also given in the table.

Atom index	Atom types	Partial charges	Atom index	Atom types	Partial charges	Atom index	Atom types	Partial charges	Atom index	Atom types	Partial charges
1	cc	0.3249	17	os	-0.2673	33	os	-0.2971	49	c3	-0.4828
2	cd	-0.5453	18	ce	-0.2875	34	c3	0.1355	50	hc	0.0958
3	ha	0.2131	19	ha	0.1540	35	h1	0.0128	51	hc	0.0958
4	cd	0.5785	20	cf	-0.1953	36	h1	0.0128	52	c3	-0.4828
5	ce	-0.7946	21	ha	0.1211	37	h1	0.0128	53	hc	0.0958
6	cg	0.5885	22	ca	-0.0075	38	c2	-0.2713	54	hc	0.0958
7	n1	-0.6116	23	ca	-0.2271	39	c3	0.4448	55	c3	0.4643
8	cg	0.5885	24	ha	0.1430	40	hc	-0.0210	56	hc	-0.0401
9	n1	-0.6116	25	ca	-0.1726	41	c3	0.4448	57	c3	0.4643
10	cd	-0.5778	26	ha	0.1276	42	hc	-0.0210	58	hc	-0.0401
11	ha	0.2085	27	ca	0.1173	43	c3	-0.4828	59	c3	-0.4442
12	cc	0.4642	28	ca	-0.1983	44	hc	0.0958	60	hc	0.0806
13	c3	-0.4888	29	cl	-0.0709	45	hc	0.0958	61	hc	0.0806
14	hc	0.1343	30	ca	0.5852	46	c3	-0.4828			
15	hc	0.1343	31	o	-0.5032	47	hc	0.0958			
16	hc	0.1343	32	ce	0.0884	48	hc	0.0958			

(a)

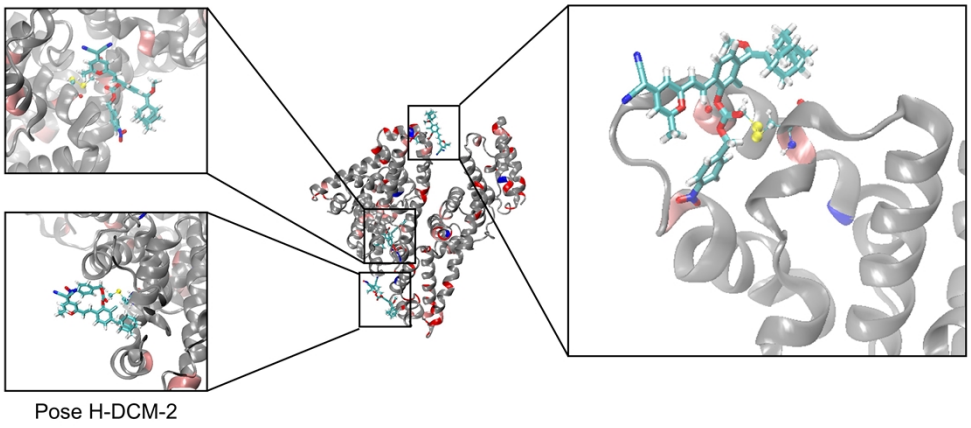

(b)

Pose	E_{BE}/ (kcal/mol)
Pose H-DCM-1	-2.08
Pose H-DCM-2	-0.71
Pose H-DCM-3	-3.14

Figure S16. Molecule calculation of DCM-SA docking with HSA. Possible binding sites (a) and their corresponding binding energies (b). Note: A cluster highlighted in red denotes the probable binding sites with the highest likelihood.

(a)

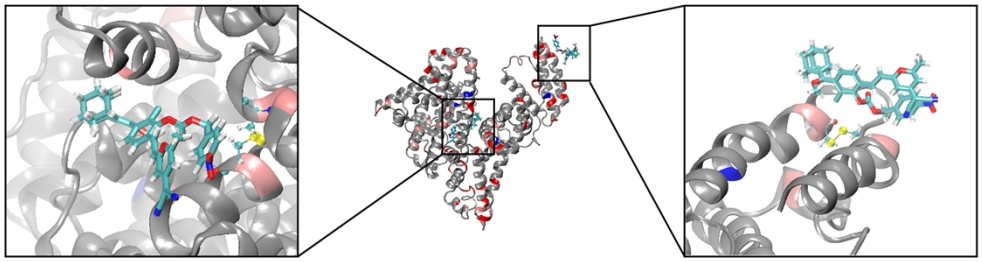

(b)

Pose	E_{BE}/ (kcal/mol)
Pose B-DCM-1	-2.73
Pose B-DCM-2	-2.04

Figure S17. Molecule calculation of DCM-SA docking with BSA. Possible binding sites (a) and their corresponding binding energies (b). Note: A cluster highlighted in red denotes the probable binding sites with the highest likelihood.

(a)

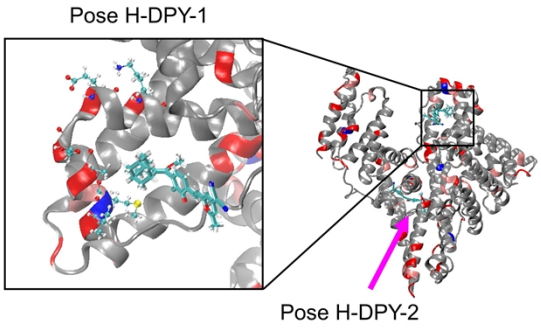

(b)

Poses	ΔH	$T\Delta S$	E_{BE}/ (kcal/mol)
Pose H-DPY-1	-33.88	-18.30	-15.58
Pose H-DPY-2	-26.89	-18.37	-8.52

Figure S18. Molecule calculation of DPY docking with HSA. Possible binding sites (a) and their corresponding binding energies (b). Note: A cluster highlighted in red denotes the probable binding sites with the highest likelihood.

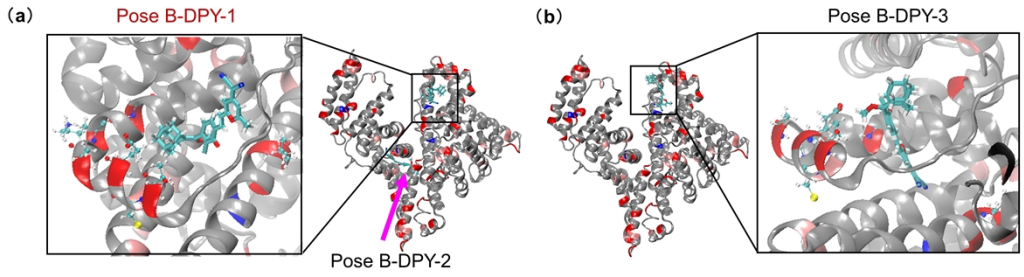

(c)

Poses	ΔH	$T\Delta S$	E_{BE}/ (kcal/mol)
Pose B-DPY-1	-36.39	-21.85	-14.54
Pose B-DPY-2	-24.58	-20.30	-4.28
Pose B-DPY-3	-24.85	-20.16	-4.69

Figure S19. Molecule calculation of DPY docking with BSA. Possible binding sites (a-b) and their corresponding binding energies (c). Note: A cluster highlighted in red denotes the probable binding sites with the highest likelihood.

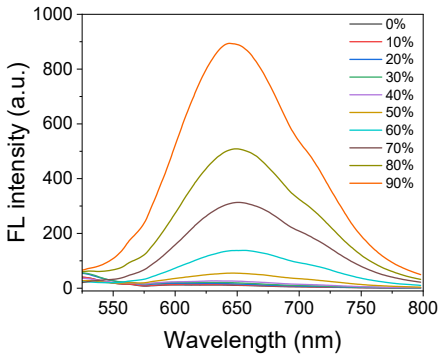

Figure S20. Fluorescence spectra of DPY (10 μM) at different glycerol ratios.

Table S4. Confirmation of DPY binding and their dissociation constants for HSA and BSA as determined by SPR.

	k_a / 1/Ms	k_d / 1/s	K_D / M
DPY+HSA	1.87e+03	9.87e-02	5.28e-05
DPY+BSA	2.54e+03	6.79e-01	2.68e-04

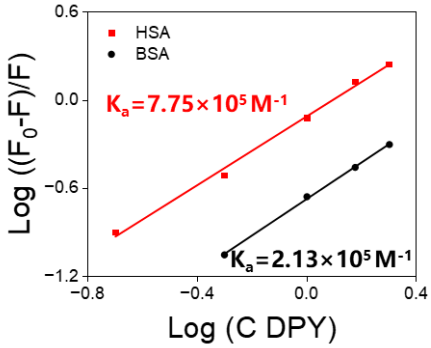

Figure S21. Calculation of the equilibrium binding constant (K_a): double-logarithm plots of HSA and BSA quenched by DPY. The equilibrium binding constant (K_a) was evaluated by the intercept of the modified Stern-Volmer Eq (log[(F_0-F)/F] = logK_a + nlog[C]). [HSA] = [BSA] = 1 μM, [DPY] = 0.2-2 μM.

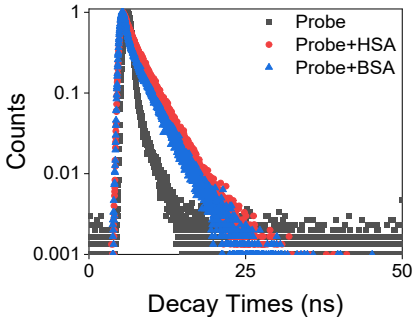

Figure S22. The steady-state fluorescence lifetime changes of DCM-SA (20 μM) before and after incubating with HSA and BSA (200 μg/mL).

Table S5. The steady-state fluorescence lifetime of DCM-SA (20 μM) in the absence and presence of HSA / BSA (200 ug/mL). $\lambda_{ex\,/\,em}$=450 nm / 640 nm.

	τ_1 / ns	τ_1 / %	τ_2 / ns	τ_2 / %	$\bar{\tau}$ / ns
Probe	0.615	87.31	2.855	12.69	1.517
Probe+HSA	2.500	90.36	5.000	9.64	2.940
Probe+BSA	1.190	40.12	3.250	58.88	2.839
DPY	0.550	71.28	2.450	28.72	1.770
DPY+HSA	1.300	19.16	2.920	80.84	2.765
DPY+BSA	1.030	28.29	2.850	71.71	2.623

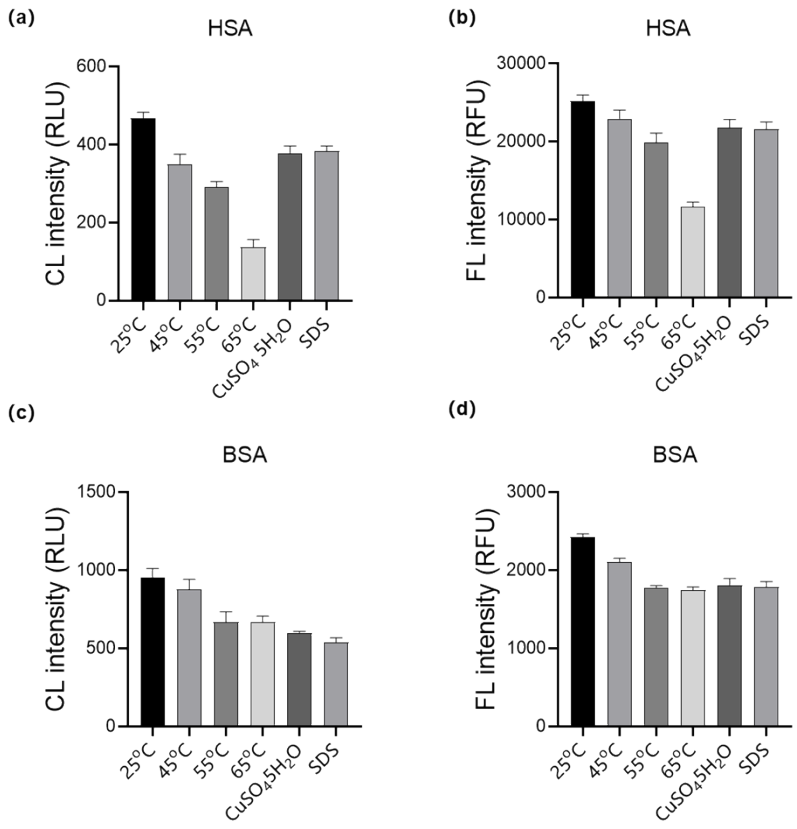

Figure S23. The chemiluminescence and fluorescence responses of DCM-SA towards pretreated albumins. Inserts: λ_{ex} = 500 nm, λ_{em} = 615 nm. Chemiluminescence intensity was obtained upon 21 mWcm^{-2} white light irradiation for 3 s. All the signals were collected by spark multimode microplate reader.

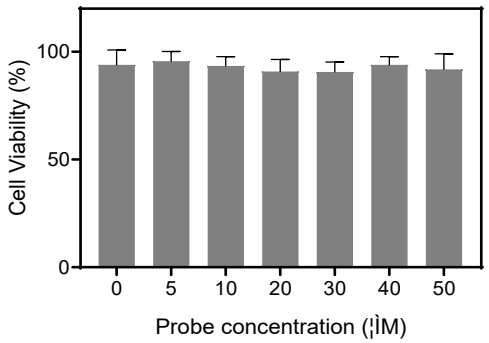

Figure S24. Percentage of viable Hepg 2 cells after treatment with different concentrations of DCM-SA for 24 h.

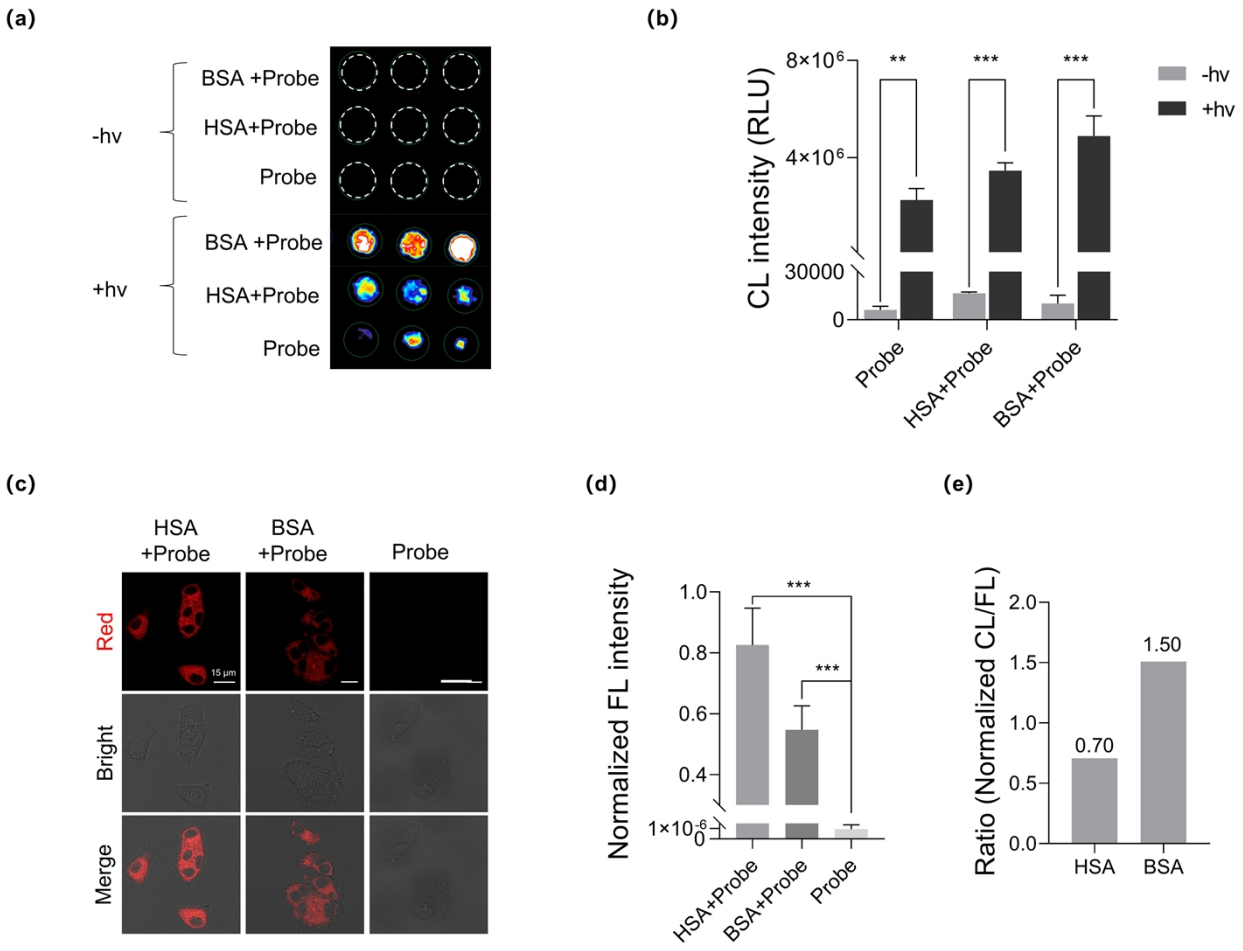

Figure S25. CL and confocal images of Hepg 2 cells. (a) CL imaging of DCM-SA (50 μM, 24 h) after pretreating with HSA (3 μM, 1 h) or BSA (3 μM, 1 h), with and without irradiation (21 mW/cm^2 for 15 s). (b) Quantification of CL signals from (a). The error bars represent the S.D. (n=3). (c) Assessing changes in SA activity in cultured cells upon treatment with HSA and BSA by fluorescence imaging. Hepg 2 cells were pretreated with HSA (3 μM, 1 h) or BSA (3 μM, 1 h) before treatment with DCM-SA (10 μM, 1 h). λ_{ex} = 500 nm, λ_{em} = 610–650 nm. Scale bar: 15 μm. (d) Quantification of FL signals from Hepg 2 cells. The error bars represent the S.D. (n=3). (e) The normalized CL/FL ratios of cells after successive incubation with HSA/BSA and DCM-SA.

Distinguishing HSA and BSA in living cells. Encouraged by the excellent albumin identification performance of DCM-SA, we further investigated its potential application in living cells. Hepg 2 cells were utilized as a bioassay model. Initially, the survival rate of Hepg 2 cells under different amounts of DCM-SA was employed to estimate the cytotoxicity. The results shown in Figure S24, over 90% Hepg 2 cells could survive well in the concentrations of DCM-SA from 0 to 50 μM, indicating probe DCM-SA possessed good bio-compatibility and negligible cytotoxicity. As expected, a conspicuous CL signal appeared in the BSA or HSA pretreatment group after irradiation, which shows significant differences compared to the control group without albumins (Figure S25a). In contrast, cells from each dark-treated group exhibited chemiluminescent signals that were almost negligible (Figure S25a and b). At the same time, cells pretreated with BSA exhibit a stronger chemiluminescent signal. As can be seen in Figure S25c, when Hepg 2 cells were loaded with probe DCM-SA (10 μM) at 37 ^{o}C for 1 h, only faint intracellular background fluorescence could be observed under confocal microscopy. In sharp contrast, when Hepg 2 cells were pretreated with HSA or BSA for 1 h, and then were incubated

with DCM-SA for 1 h, a notable enhancement in fluorescence images was observed (Figure S25d). Moreover, cells pretreated with HSA exhibit a stronger fluorescence signal. Notably, the normalized CL/FL ratio of cells treated with HSA is 0.70, falling within the range of 0 to 0.8. In contrast, the ratio for cells treated with BSA exceeds 0.8, aligning with prior experimental findings (Figure S25e). All these results provide strong support that DCM-SA can be utilized for specific and sensitive imaging and discrimination of exogenous HSA and BSA in live cells.

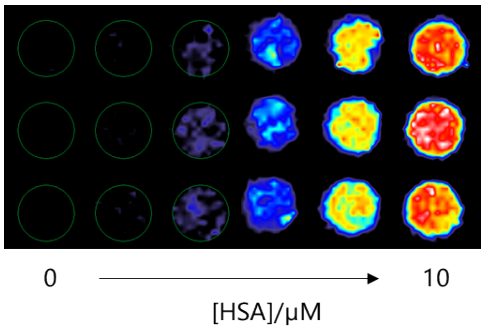

Figure S26. CL imaging of DCM-SA vs HSA concentration.

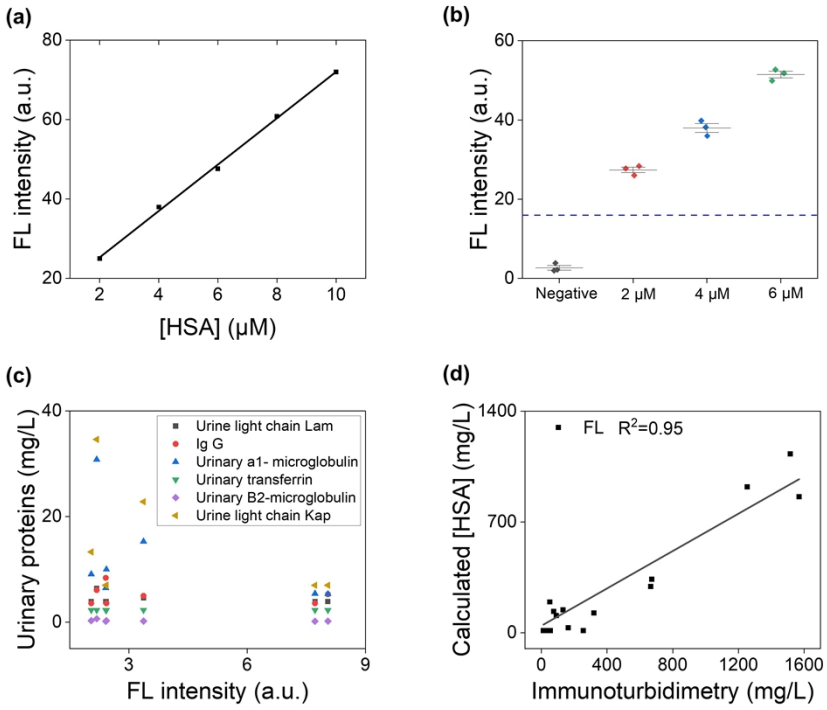

Figure S27. (a) Fluorescence intensities of DCM-SA (10 μM) as a function of [HSA] (0–10 μM). (b) Fluorescence intensities of urine from four healthy volunteers after incubation with a certain concentration of HSA at 615 nm. (c) The relationship between the fluorescence intensity detected by DCM-SA of urine from patients with normal HSA levels and elevated levels in 6 additional urinary immunity indexes. (d) Comparison of the concentration of HSA in urine samples determined by immunoturbidimetry and DCM-SA-based analysis in fluorescence mode. Note: Benefitting from HSA-selective hydrolysis response, DCM-SA exhibits no correlation between the fluorescence signal and the concentrations of other urinary proteins.

4. ^{1}H NMR Spectra, ^{13}C NMR Spectra, and HRMS Spectra

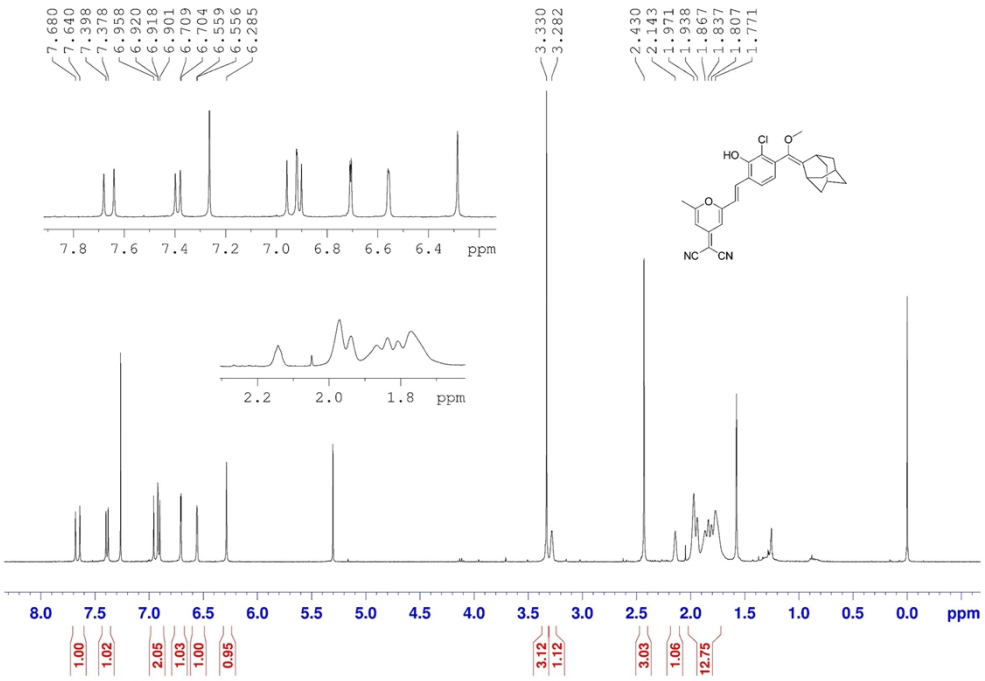

Figure S28. ^{1}H NMR spectrum of **DPY** in $CDCl_3$.

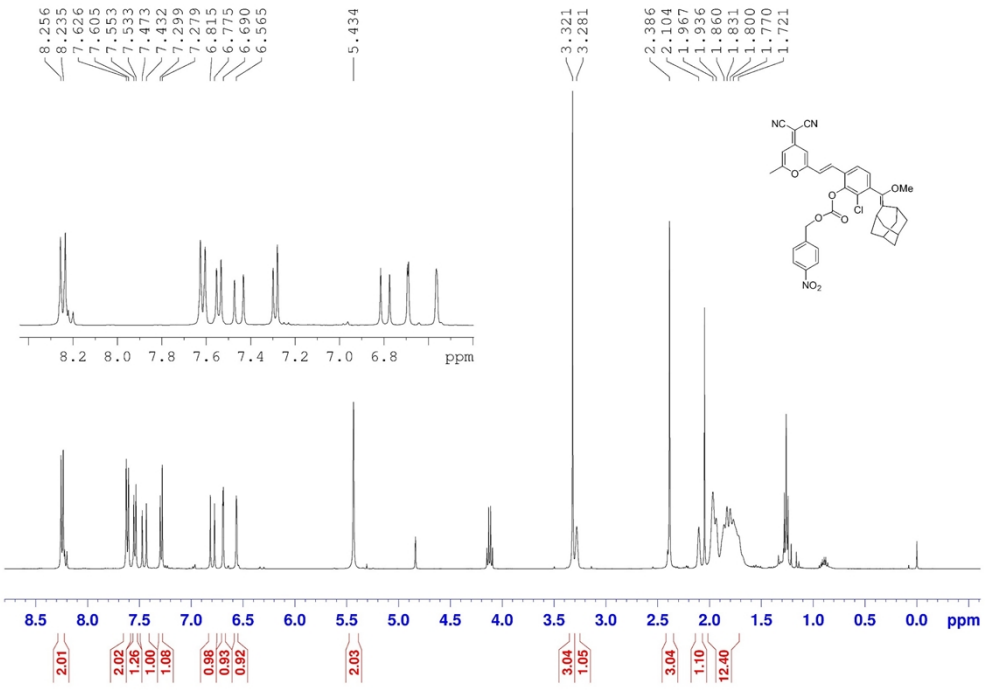

Figure S29. ^{1}H NMR spectrum of **DCM-SA** in $CDCl_3$.

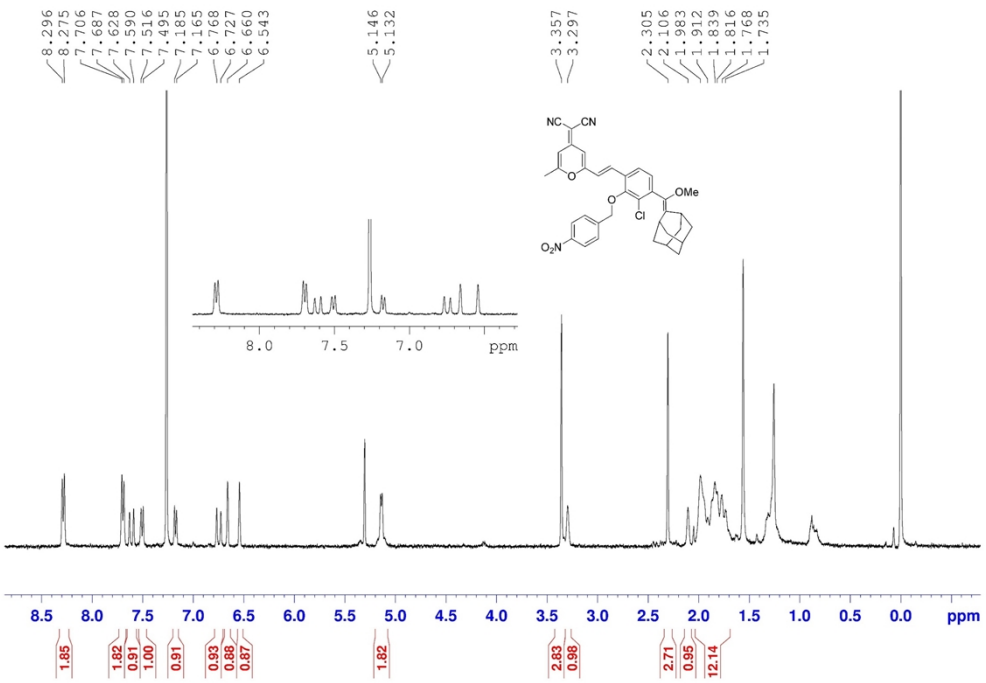

Figure S30. ^{1}H NMR spectrum of **CF-Cl-NB** in $CDCl_3$.

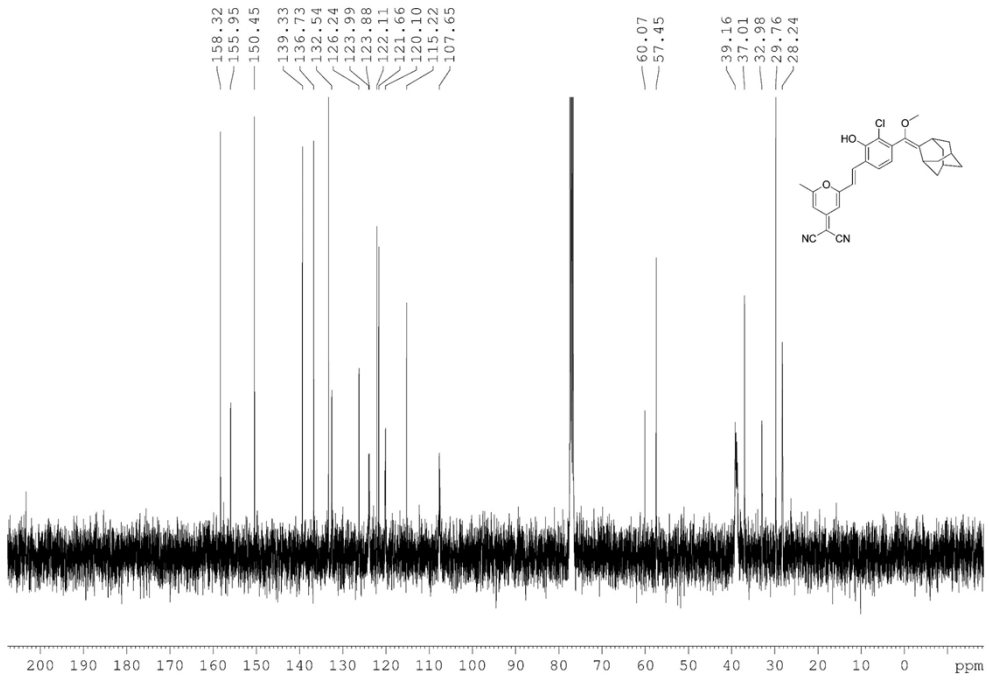

Figure S31. ^{13}C NMR spectrum of **DPY** in $CDCl_3$.

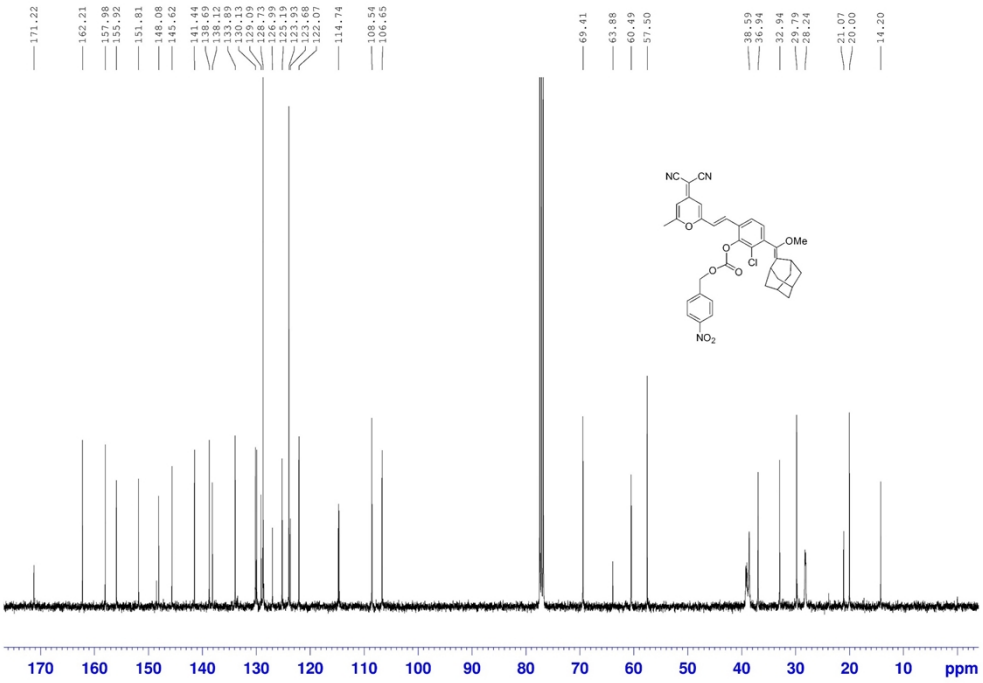

Figure S32. ^{13}C NMR spectrum of **DCM-SA** in $CDCl_3$.

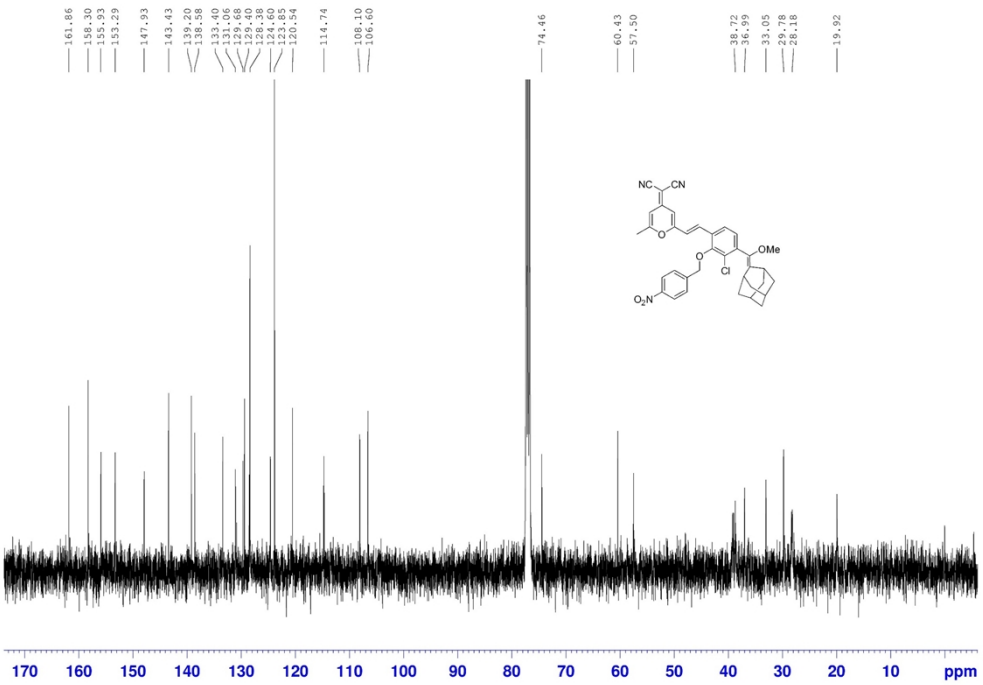

Figure S33. ^{13}C NMR spectrum of **CF-Cl-NB** in $CDCl_3$.

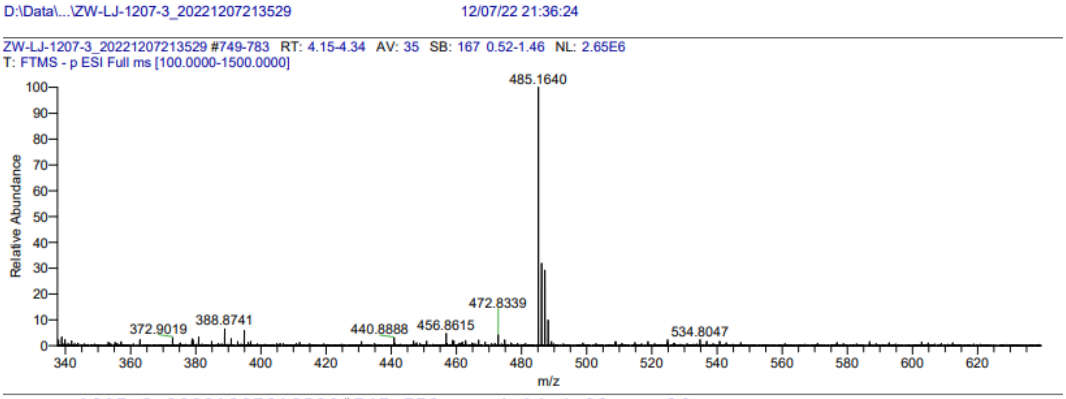

ZW-LJ-1207-3_20221207213529#747-772 RT: 4.14-4.28 AV: 26
T: FTMS - p ESI Full ms [100.0000-1500.0000]
m/z= 483.95-486.07

m/z	Intensity	Relative	Theo. Mass	Delta (ppm)	Composition
485.1642	3019613.8	100.00	485.1626	1.53	$C_{29}H_{26}O_3N_2Cl$

Figure S34. HR-MS spectrum of **DPY**.

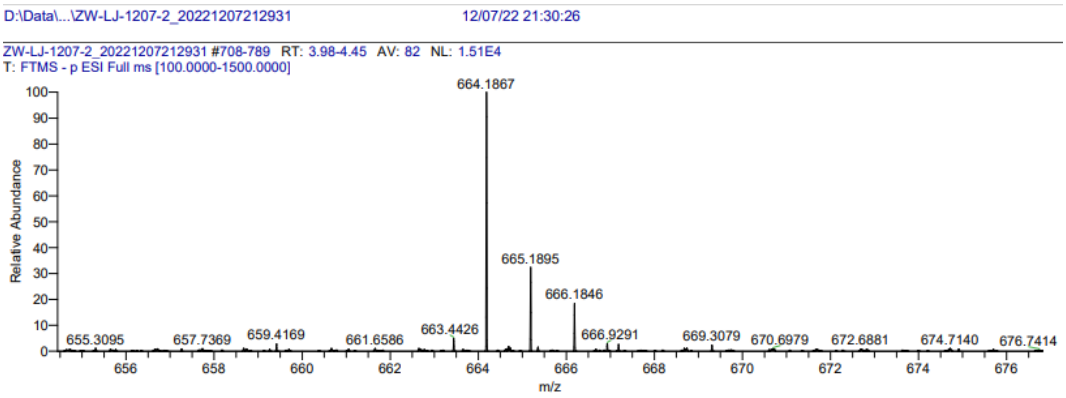

ZW-LJ-1207-2_20221207212931#713-792 RT: 4.01-4.47 AV: 80
T: FTMS - p ESI Full ms [100.0000-1500.0000]
m/z= 664.03-664.34

m/z	Intensity	Relative	Theo. Mass	Delta (ppm)	Composition
664.1867	15202.8	100.00	664.1845	2.21	$C_{37}H_{31}O_7N_3Cl$

Figure S35. HR-MS spectrum of **DCM-SA**.

Elemental Composition Report **Page 1**

Single Mass Analysis
Tolerance = 15.0 PPM / DBE: min = -1.5, max = 50.0
Element prediction: Off
Number of isotope peaks used for i-FIT = 3

Monoisotopic Mass, Even Electron Ions
227 formula(e) evaluated with 1 results within limits (up to 50 closest results for each mass)
Elements Used:
C: 0-36 H: 0-32 N: 0-3 O: 0-5 Na: 0-1 Cl: 0-2 K: 0-1
WH-ZHU
ZW-LJ-31228 151 (1.725) Cm (146:151)

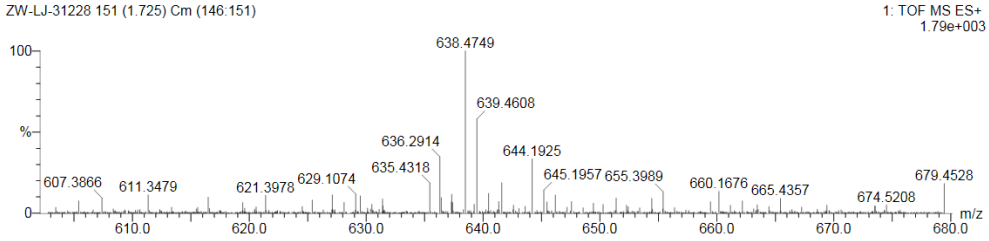

Minimum:				-1.5								
Maximum:		5.0	15.0	50.0								
Mass	Calc. Mass	mDa	PPM	DBE	i-FIT	i-FIT (Norm)	Formula					
644.1925	644.1928	-0.3	-0.5	21.5	142.4	0.0	C36	H32	N3	O5	Na	Cl

Figure S36. HR-MS spectrum of **CF-Cl-NB**.